Science of Sintering, **53** (2021) 267-283

https://doi.org/10.2298/SOS2102267G

UDK: 546.831; 546.824; 622.785

Effect of TiO_2 in Fine Zircon Sintering and Properties

Matías R. Gauna[1,2*)], Juan M. Martinez[1,3], María S. Conconi[1,3], Gustavo Suárez[1,3], Nicolás M. Rendtorff[1,3]

[1]CETMIC. Centro de Tecnología de Recursos Minerales y Cerámica (CIC-CONICET La Plata-UNLP) Cno. Centenario y 506 M.B. Gonnet (1897), Buenos Aires, Argentina.

[2]Departamento de Construcciones, Facultad de Ingeniería, Universidad Nacional de La Plata, 1 y 47, La Plata (1900), Buenos Aires, Argentina.

[3]Departamento de Química, Facultad de Ciencias Exactas, Universidad Nacional de La Plata, 47 y 115, La Plata (1900) Buenos Aires, Argentina.

Abstract:

The effect of the TiO_2 addition in the ceramic processing of dense zircon materials from zircon fine powders was established. The addition of TiO_2 (5-10 wt%) permitted to obtain dense ceramics at lower temperatures (100-150 ^oC below), with comparable mechanical behavior. The thermochemical processes were described after a multi-technique experimental approach, which included a sintering analysis, powder X-Ray diffraction analysis (XRD), scanning electronic microscopy (SEM) and Vickers hardness of the polished dense obtained ceramics. After 1400 ^oC heating programs, the added TiO_2 acts as a sintering aid with no important chemical reactions, and presented improved mechanical behavior in comparison with pure zircon ceramics. On the other side, in samples fired at 1500 ^oC, TiO_2 partially (≈50 %) reacts with zircon, forming $ZrTiO_4$, while the formed SiO_2 goes to the grain boundaries. Samples with 5 wt% TiO_2 present better mechanical behavior than the ones with 10 wt%. The performed mechanical characterization indicates the merits of the material processed by this inexpensive processing route. Developed density, hardness (≈10 GPa) and fracture toughness (≈2 $MPa.m^{-1/2}$) are comparable with the best figures reported.

***Keywords**: Zircon; TiO_2; Processing; Sintering; Properties.*

1. Introduction

It is well known that zircon ($ZrSiO_4$) materials are good refractories for high temperature uses, due to zircon's chemical stability, low thermal conductivity, low thermal expansion and corrosion resistance, among others properties [1–5].

Zircon materials are used in glass and steel industries [5, 6] especially because of pure zircon undergoes no major structural changes below 1680 ^oC, temperature at which it dissociates into zirconia and silica. The decomposition temperature decreases with the presence of impurities or mechanical pretreatments [1]. Due to their high refractoriness, zircon powders are difficult to sinter. To overcome this drawback, some additives are usually employed as sintering aids; the typical additives include, for example, refractory clays and titania (TiO_2) [7]. Although beneficial for sintering, sometimes the incorporation of these additives results in the loss of some of zircon's distinctive properties.

*) **Corresponding author:** mgauna@cetmic.unlp.edu.ar

Generally, dense zircon ceramics without additives are processed by advance sintering techniques such as hot pressing [8, 9] or spark plasma sintering (SPS) [10, 11]. On the other side, it has been reported that the mechanochemical activation by high energy ball milling is a suitable pretreatment for raw materials in the obtention of dense ceramics. Its goal is to activate the chemical and physical processes by incorporating surface energy powders that are usually nanosized, thus effectively achieving homogeneous mixtures of powders, even if they differ in particle size [12–14]. Sintering is one of these processes activated by high energy milling.

The first attempt to study the mechanical activation of zircon was reported by Motoi [15]. It was demonstrated that prolonged ball milling not only causes particle size reduction but also amorphizes the mineral, which leads to partial decomposition into ZrO_2 and SiO_2 and can also enhance solubility in fluorhidric acid.

The milling effect on the zircon alumina reaction sintering for obtaining mullite zirconia refractory composites was also studied [16, 17].

In particular, the mechanical behavior of this kind of material is of technological interest, and is related to the microstructure, phase composition and sintering grade. Suarez et al. reported the effect of colloidal processing optimization by slip casting of highly concentrated aqueous dispersions on the sintering of dense zircon ceramics [18]. In other work, Rendtorff et al. studied the effect of milling for a nonconventional advance sintering method (SPS) and the mechanical properties of dense zircon ceramics were reviewed and compared [10].

In a prior work we presented a systematic study of the effect of high energy milling treatment and the subsequent direct sintering of pure zircon fine powder [14]. Although there weren`t changes in the morphology of the activated powders, observed by SEM, they sintered after thermal treatment at 200 ^oC below the un-milled powders [14]. XRD allowed the identification of an incipient partial dissociation of zirconium silicate after long term (60-120 minutes) high energy milling treatments. This slight dissociation was also observed after the thermal treatments of the studied powders.

The introduction of TiO_2 is expected to promote the sintering of zircon. The ternary phase diagram ZrO_2-SiO_2-TiO_2 suggests that TiO_2 could react with ZrO_2 to form $ZrTiO_4$ [19–21].

Zirconium titanate ($ZrTiO_4$) is commonly used as a dielectric in microwave devices due to its high permittivity to microwave frequencies [22]. $ZrTiO_4$ has been proposed for structural applications at severe thermomechanical conditions [20, 21], and in composite structural ceramics [23, 24]. The introduction of zirconia particles imbibed in structural ceramics has proven to result in several reinforcement mechanisms [25, 26]. This strategy has been proposed and studied for zircon based materials [11, 27].

To our knowledge, no systematic TiO_2 addition study has been carried out. The main objective of this work is to establish the effect of the TiO_2 addition in the ceramic processing of dense zircon ceramics, from fine zircon powders. For this, a systematic formulation-processing-properties study was carried out. The high energy milling pretreatment has proven to enhance sintering processes [14], which was assessed as well. Particularly sinter parameters, developed phases, microstructure and mechanical properties were studied and correlated.

2. Materials and Experimental Procedures

2.1 Materials and methods

A commercial zircon ($ZrSiO_4$) powder (Kreutzonit Super Extra Weiß, Mahlwerke Helmut Kreutz GmbH, Germany, 0.8 μm) and anatase (TiO_2) powder (Cicarelli, Argentina) were used (Z and T respectively). Two powder mixtures were prepared adding 5 and 10 wt%

of additive (ZT). They were mixed in a planetary mill (HEBM) (Pullverizer 7 Premium Line, Fritsch Co., Ltd., Germany) at 350 rpm for 3 min for homogenization of the unmilled mixtures, and at 850 rpm for 60 min for the milled ones (Table I). The same treatment was performed for pure zircon powder (Z). Zirconia jars of 85 ml were used and 60 g of zirconia balls (10 mm diameter) as mill and milling media respectively; 6 g of powder were used in each batch, dispersed in ethanol [11, 14, 28].

X-ray diffraction (XRD-Bruker D2 phaser Cu-Kα incident radiation at 30 kV to 10 mA) performed at 2θ between 15 and 80° was used to evaluate the effect of the milling time on the crystalline phases. Rietveld refinement was performed in order to follow the possible partial zircon dissociation and zirconium titanate formation [28–30].

Disc-shaped samples of 15 mm diameter were prepared from dried and screened (mesh 100) powders; these were first uniaxially pressed at 25 MPa and then isostatically pressed at 100 MPa [31, 32]. Afterwards, samples were fired at 1300, 1400 and 1500 ^{o}C in an electric furnace. The employed heating and cooling rate were both, in all cases, 5 ^{o}C.min^{-1} with a holding time of 2 hours (Table I).

Tab. I Powders mixtures and obtained ceramic samples according to additive employed, milling time and sintering temperature.

Sample (powders)	Sample (ceramics)	Additive TiO_2 (T) (% weight)	Milling time (minutes)	Sintering temperature (^{o}C)
Z-0	**Z-0-14**	0	0	1400
	Z-0-15	0	0	1500
Z-60	**Z-60-14**	0	60	1400
	Z-60-15	0	60	1500
ZT5-0	**ZT5-0-13**	5	0	1300
	ZT5-0-14	5	0	1400
	ZT5-0-15	5	0	1500
ZT5-60	**ZT5-60-13**	5	60	1300
	ZT5-60-14	5	60	1400
	ZT5-60-15	5	60	1500
ZT10-0	**ZT10-0-13**	10	0	1300
	ZT10-0-14	10	0	1400
	ZT10-0-15	10	0	1500
ZT10-60	**ZT10-60-13**	10	60	1300
	ZT10-60-14	10	60	1400
	ZT10-60-15	10	60	1500

Sintered disc shape samples were characterized by diametral shrinkage and textural properties – open porosity and apparent density – were obtained by the Archimedes method, using distilled water. Evolution of the crystalline phases composition with sintering temperature was evaluated by X-ray diffraction (XRD-Bruker D2 phaser Cu-Kα incident radiation at 30 kV to 10 mA) and Rietveld refinement [28, 29, 33].

To assess the densification of the composite the theoretical density (D_{Theo}) of the composite was estimated through the following Equation:

$$D_{Theo} = \sum_{i=0}^{n} V_i \times D_i \qquad (1)$$

where V_i is the volume fraction of each crystalline phase (i) evaluated by XRD-Rietveld quantification and D_i is the theoretical density of each phase.

Developed microstructures were evaluated by scanning electron microscopy (SEM-JEOL JCM-6000, Japan). Finally, Vickers hardness was evaluated (Buhhler Indentament 1100, USA) by, at least, ten indents under 3 Kg load and 15 second dwelling time [14]. Fracture toughness (K_{IC}) was determined by measuring the cracks generated by indentation via Evans and Charles method [34], using the formula proposed showed in Equation 2.

$$K_{IC} = 0{,}16\ H\, a^{0.5} \left(\frac{c}{a}\right)^{-1.5} \qquad (2)$$

where H is Vickers hardness; a is the semi diagonal of the indentation and c is the distance from the center of the indentation to the tip of the crack.

3. Results and Discussion

3.1 Powder milling pretreatment, effect of the TiO_2 addition

The effect of milling on pure zircon fine powders has been previously studied [14]; showing a notorious enhancement of the sinterability of these powders accompanied by a slight zircon dissociation (Equation 3) and the absence of important changes in grain morphology or grain size distribution. It can be presumed that the performed milling process (in ethanol) improves the homogenization of these fine powder mixtures.

$$ZrSiO_4 \leftrightarrow (m - t - c)\, ZrO_2 + SiO_2\ (Glassy) \qquad (3)$$

Figs. 1a and 1b compare the XRD patterns of the powders before and after the HEBM with 5 and 10 wt% of additive respectively (ZT) with the milled powder of zircon Z-60. The ZT unmilled mixtures show only zircon and anatase (TiO_2) phases [35]. No broadening of the peaks is observed, showing that the pretreatment did not affect the phases crystallinity. At the same time, the inset in this figure shows the main peaks of the zirconia phase (tetragonal and/or cubic) [28], showing a clear evidence of the incipient silicate dissociation in the milled powders according the Equation 3.

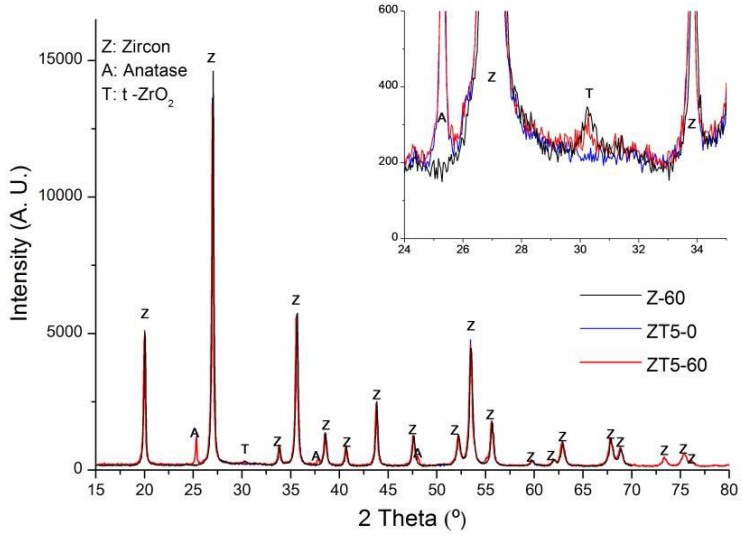

Fig. 1a. XRD patterns of the powders before (ZT5-0) and after (ZT5-60) the HEBM with 5 wt% of additive (TiO_2) with the milled powder of alone zircon (Z-60). (Inset: main zirconia phases peaks) [28].

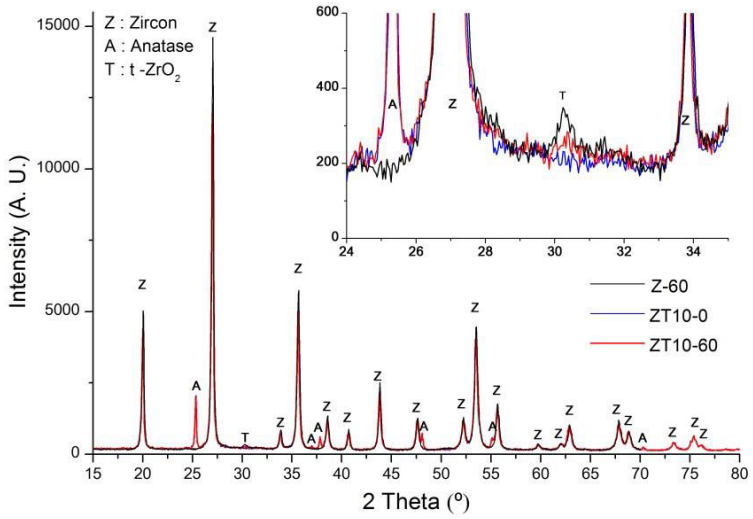

Fig. 1b. XRD patterns of the powders before (ZT10-0) and after (ZT10-60) the HEBM with 10 wt% of additive (TiO_2) with the milled powder of alone zircon (Z-60). (Inset: main zirconia phases peaks) [28].

3.2 Thermal treatment of the powder mixtures

3.2.1. Sintering parameters: Shrinkage, apparent density and open porosity as a function of the processing variables

Table II shows the milling and sintering temperature effect on the textural properties, theoretical density (D_{Theo}), apparent density, open porosity and linear shrinkage of the obtained zircon samples. The open porosity is the most illustrative sintering parameter.

In general, HEBM improved sintering for all samples when compared to its unmilled par (at same sintering temperature and TiO_2 addition). Also, TiO_2 addition resulted in lower porosity values/enhanced sintering when compared with samples at same sintering temperature and no TiO_2.

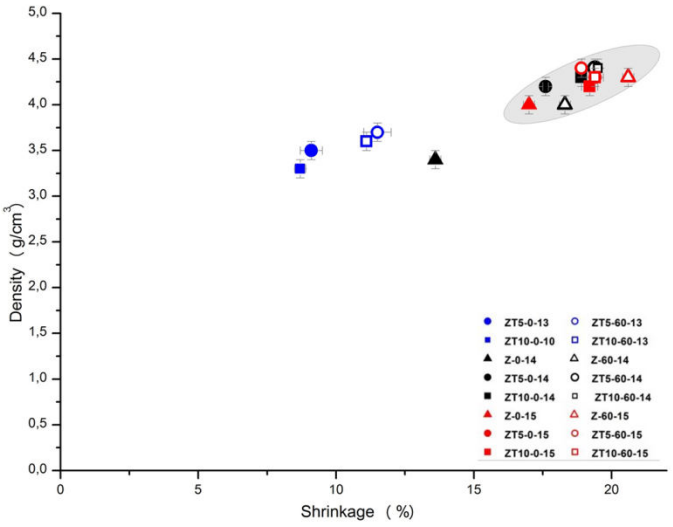

Fig. 2. Correlation between the sintering parameters, apparent Density (g/cm^3) as a function of Shrinkage (%) of the studied zircon based materials.

After 1300 °C treatments pure samples do not sinter, sintering occurs after equivalent thermal treatments in the TiO_2 added samples; particularly 10 wt% additions result in a slight higher sintering than the 5 wt% addition. After 1400 °C treatments, the pure sample presents a certain grade of sintering enhanced by the milling pretreatment and the additive samples are fully sintered. Moreover, after 1500 °C treatments the only not fully sintered sample is the unmilled pure zircon sample (Z-0-15), which presents 8 % porosity.

It could be stated that the addition of TiO_2, reduces sintering temperatures and allows the possibility of obtaining zircon ceramics with similar textural properties than pure ones. Achieved densities are in all the cases below pure zircon's theoretical density (4.56 $g.cm^{-3}$), being these differences explained in term of the presence of lighter phases (TiO_2, SiO_2), close porosity, and partial dissociation. Nevertheless, density is expectably correlated with shrinkage and open porosity, as shown in Fig. 2, thus proving that, any of them could be employed as sintering parameter.

Tab. II Diametral shrinkage, theoretical density, apparent density and open porosity of sintered ceramics. (SD: Standard deviation).

Sample	$T_{sint.}$ (°C)	Shrinkage (%)	SD	Theoretical Density ($g.cm^{-3}$)	Apparent Density ($g.cm^{-3}$)	SD	Open Porosity (%)	SD
Z-0-13	**1300**	Not sintered						
Z-60-13	**1300**	Not sintered						
ZT5-0-13	**1300**	9.1	0.4	4.5	3.5	0.1	25.6	0.5
ZT10-0-13	**1300**	8.7	0.2	4.5	3.3	0.1	26.0	0.4
ZT5-60-13	**1300**	11.5	0.5	4.5	3.7	0.1	22.3	0.5
ZT10-60-13	**1300**	11.1	0.2	4.5	3.6	0.1	22.0	0.4
Z-0-14	**1400**	13.6	0.2	4.6	3.4	0.1	23.0	0.2
Z-60-14	**1400**	18.3	0.2	4.6	4.0	0.1	11.1	0.3
ZT5-0-14	**1400**	17.6	0.1	4.5	4.2	0.1	0	-
ZT10-0-14	**1400**	18.9	0.1	4.5	4.3	0.1	0	-
ZT5-60-14	**1400**	19.4	0.2	4.5	4.4	0.1	0	-
ZT10-60-14	**1400**	19.5	0.1	4.5	4.4	0.1	0	-
Z-0-15	**1500**	17.0	0.2	4.6	4.0	0.1	8.5	0.3
Z-60-15	**1500**	20.6	0.2	4.6	4.3	0.1	0	-
ZT5-0-15	**1500**	19.4	0.3	4.6	4.3	0.1	0	-
ZT10-0-15	**1500**	19.2	0.3	4.6	4.2	0.1	0	-
ZT5-60-15	**1500**	18.9	0.1	4.6	4.4	0.1	0	-
ZT10-60-15	**1500**	19.4	0.2	4.6	4.3	0.1	0	-

3.2.2. Crystalline phases developed after the heating treatment

The crystalline phases determination after the different sintering treatments was performed by XRD. Fig. 3a compares XRD patterns of sintered ceramics under thermal treatments of 1400 and 1500 °C from zircon powders with and without milling (Z-60 and Z-0 respectively). The inset in this figure shows the main peaks of the zirconia phase (monoclinic, tetragonal and/or cubic) evidencing higher zirconium silicate dissociation in the sintered ceramic at 1500 °C obtained from milled powder.

Fig. 3b compares XRD patterns of sintered ceramics under thermal treatment of 1300, 1400 and 1500 °C obtained from mixtures with 10 wt% additive. At 1300 and 1400 °C the diffraction peaks of zircon and rutile phases are observed; at 1500 °C the diffraction peaks corresponding to the srilankite phase ($ZrTiO_4$) are also observed. Anatase (A) was completely transformed to rutile (R) due to the thermal treatment, as shown in Equation 4.

$$ZrSiO_4\ (Z) + TiO_2(A) \leftrightarrow\ ZrSiO_4\ (Z) +\ TiO_2\ (R) \quad (4)$$
$$ZrSiO_4\ (Z) +\ TiO_2\ (R) \leftrightarrow ZrTiO_4\ (S) +\ SiO_2\ (G: glassy) \quad (5)$$

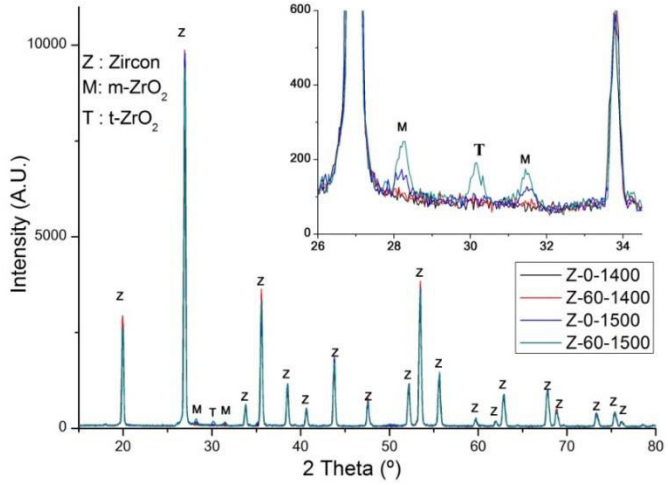

Fig. 3a. XRD patterns of sintered ceramics under thermal treatment of 1400 and 1500 °C obtained from Z-0 and Z-60 powders.

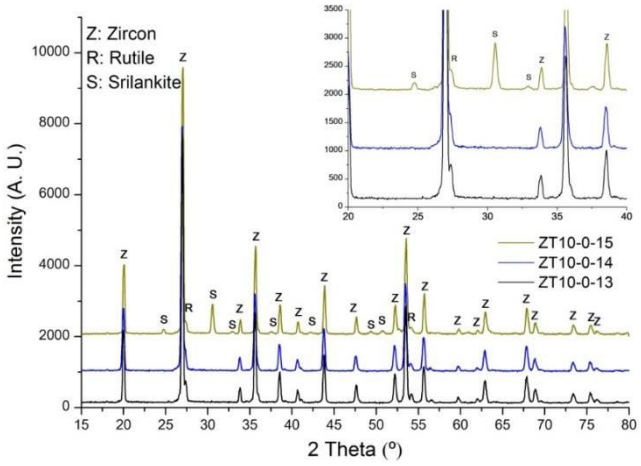

Fig. 3b. XRD patterns of sintered ceramics under thermal treatment of 1300, 1400 and 1500 °C obtained from mixtures with 10 wt% of TiO_2.

Fig. 4 compares the XRD patterns of the sintered ceramics obtained at 1500 °C before and after the HEBM with 5 and 10 wt% of additive. Zirconium silicate is the main crystalline phase in all studied samples, with no important changes in the cell parameters in all the refined structures, showing that there is no detectable ion interfusion or solid solution. All XRD patterns also show diffraction peaks corresponding to the srilankite phase ($ZrTiO_4$). Table III shows the quantification of crystalline phases (zircon, rutile and srilankite) by Rietveld method for all sintered ceramics. Samples sintered at 1500 °C show the presence of srilankite phase. No crystalline silica phases (quartz, cristobalite or tridymite) were detected; presumably, the produced SiO_2 is forming in the grain boundaries as a glassy phase. The resulting values of the R_{wp} parameters were in all cases adequate and below 17.

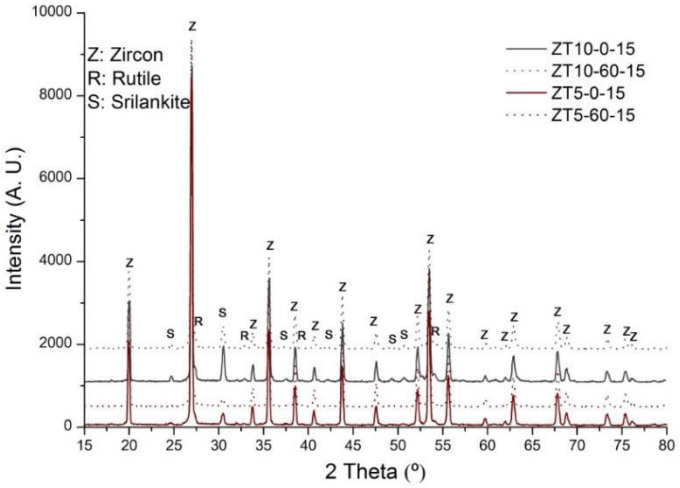

Fig. 4. XRD patterns of sintered ceramics at 1500 °C obtained from the powders before and after the HEBM with 5 and 10 wt% of TiO_2.

Tab. III Quantification results of the sintered ceramics applying the Rietveld method.

Sample	$ZrSiO_4$ (wt %)	SD	r-TiO_2 (wt %)	SD	$ZrTiO_4$ (wt %)	SD	m-ZrO_2 (wt %)	SD	t-ZrO_2	SD
Z-0-14	100	-	-	-	-	-	-	-	-	-
Z-60-14	100	-	-	-	-	-	-	-	-	-
Z-0-15	97.6	0.5	-	-	-	-	2.4	0.1	-	-
Z-60-15	95.1	0.4	-	-	-	-	3.7	0.1	1.25	0.1
ZT5-0-13	95.3	0.5	4.7	0.3	-	-	-	-	-	-
ZT5-0-14	93.2	0.5	6.8	0.3	-	-	-	-	-	-
ZT5-0-15	92.0	0.5	2.7	0.2	5.3	0.1	-	-	-	-
ZT5-60-13	94.8	0.5	5.2	0.2	-	-	-	-	-	-
ZT5-60-14	95.0	0.5	5.1	0.2	-	-	-	-	-	-
ZT5-60-15	93.8	0.5	2.8	0.1	3.4	0.1	-	-	-	-
ZT10-0-13	90.8	0.5	9.2	0.3	-	-	-	-	-	-
ZT10-0-14	88.0	0.5	12.0	0.3	-	-	-	-	-	-
ZT10-0-15	82.9	0.5	5.0	0.3	12.1	0.1	-	-	-	-
ZT10-60-13	89.8	0.4	10.2	0.3	-	-	-	-	-	-
ZT10-60-14	90.2	0.5	9.8	0.3	-	-	-	-	-	-
ZT10-60-15	84.8	0.5	6.0	0.3	9.2	0.1	-	-	-	-

Fig. 5 shows the crystalline phases after the processing route employed as a function of the three different variables that were explored: milling pretreatment [14]; TiO_2 addition (0-10 wt%), and sintering temperature (1300-1500 °C). Samples fired at 1300 °C were not completely sintered (see Fig. 5); on the other side, samples fired at 1400 and 1500 °C are fully sintered. In all cases, the principal crystalline phase is zirconium silicate, which is accompanied by the described phases. For samples fired at 1300 and 1400 °C, the quantified (unreacted) TiO_2 in the sintered samples is similar to the initially incorporated in the formulations: ≈ 5 and ≈ 10 wt%, and the milling pretreatment effect is not relevant. For samples fired at 1500 °C the described thermochemical processes (Equations 4 and 5), were observed with a partial advance (≈ 50 %), and unreacted TiO_2 was observed in both ZT5 and ZT10 samples with and without milling treatment.

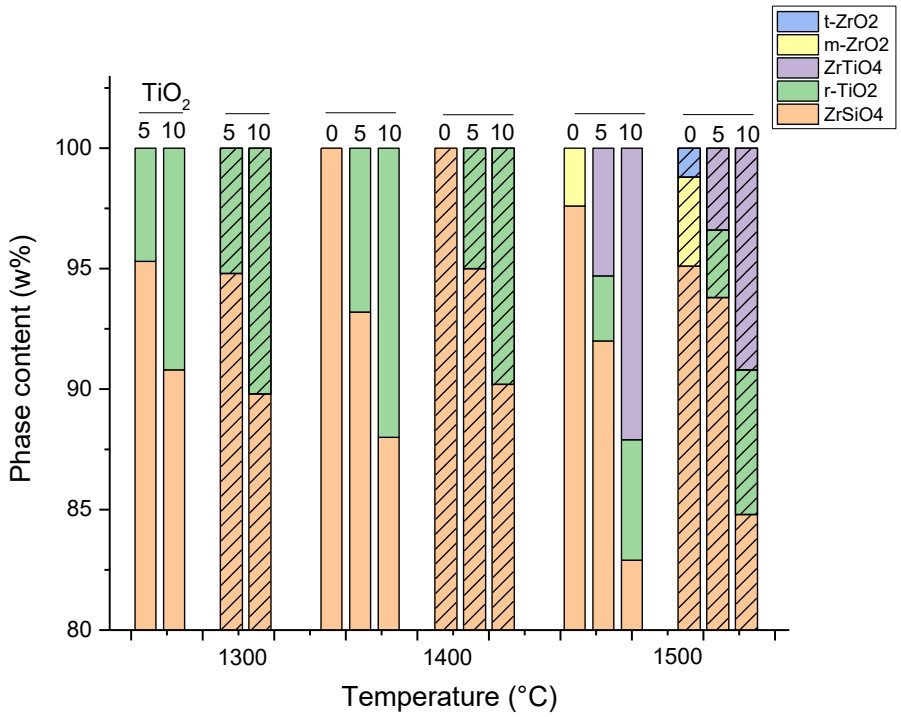

Fig. 5. Developed crystalline phases weight content of the sintered samples (milled and unmilled) as a function of the sintering temperature (1300-1500 °C) and initial TiO_2 proportion (0-10 wt%). (milled samples, with diagonal stripes*)

3.2.3. Developed microstructure by scanning electron microscopy (SEM)

The processes of pure zircon materials in an equivalent route were previously described [14]. We intend to describe the effect of the TiO_2 addition, milling pretreatment and sintering maximum temperature. SEM images of the gold coated polished surfaces were analyzed (Figs 6 and 7). Dense homogenous microstructures were observed in all ceramics developed.

The effect of the milling pretreatment and sintering temperature on the 5 wt% added samples is analyzed in Fig. 6. It shows the ZT5-0-14, ZT5-60-14, ZT5-0-15 and ZT5-60-15 sintered samples. Images "a" and "c" belong to ceramics obtained from unmilled powders, and images "b" and "d" from the milled ones. Dense homogeneous microstructures are generally obtained by the chosen processing route, the TiO_2 addition assure, in all the cases, the correct sintering of zircon powders. Fine grain size and rounded grains are observed. This

is explained by the previous milling treatment; some grain growth is observed as well, comparing grain size with starting powders diameters. The isostatic pressing results in high but not necessarily full compaction of the fine powders Because of this, some micropores (some microns in size) can be observed in all the microstructures.

As observed by XRD, TiO_2 incorporation resulted in a partial $ZrSiO_4$ dissociation, followed by $ZrTiO_4$ formation. This results in the formation of a SiO_2 based glassy phase that imbibe the silicate grains, observed in the grain border as a darker phase in Fig. 7a, as in similar systems. $ZrTiO_4$ grains appear in a lighter gray color marked with an S. No important differences were observed with or without the milling treatment at 1500 ^oC.

Compared with the ceramics obtained from zircon without additives using the same heat treatment and milling time, an improved microstructure is observed (porosity near null and density near 4.2-4.4 $g.cm^{-3}$) [14] with the addition of TiO_2 in the studied proportions. The developed microstructure allowed the evaluation of the Vickers hardness. As it can be seen, all materials present expected micro pores (closed apparently) considering the processing route; and the open porosity was shown to be close to zero.

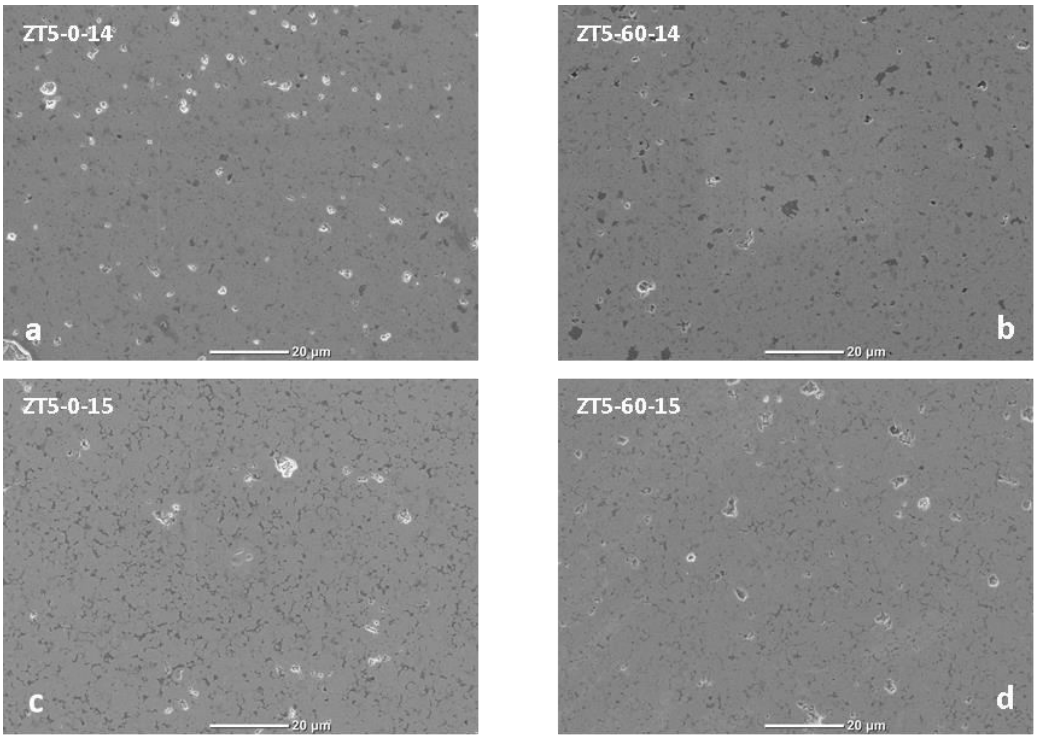

Fig. 6. SEM images of zircon sintered ceramics with 5 wt% of TiO_2 (X500 magnification).

Fig. 7 presents a group of micrographs showing the effect of the addition of TiO_2 at 1500 ^oC. The samples correspond to the ones presented in Fig. 6c and 6d (ZT5-0-15, ZT5-60-15) but now compared with the ZT10-0-15, ZT10-60-15 with 10 wt% of Titania addition. The images demonstrate that a high sintering was achieved for all ceramics.

Detected phases are in concordance with XRD, analysis (Table III). Dense zircon (Z) materials with the presence of some pores (P) as well as some imbibed srilankite (S) grains and glassy (G) grain boundaries can be observed (phases were corroborated by EDS punctual analysis). This fact is a merit of the processing route. Several larger zircon rounded grains are observed (diameters over 5 µm), which is expected to occur at higher temperatures (1500 ^oC).

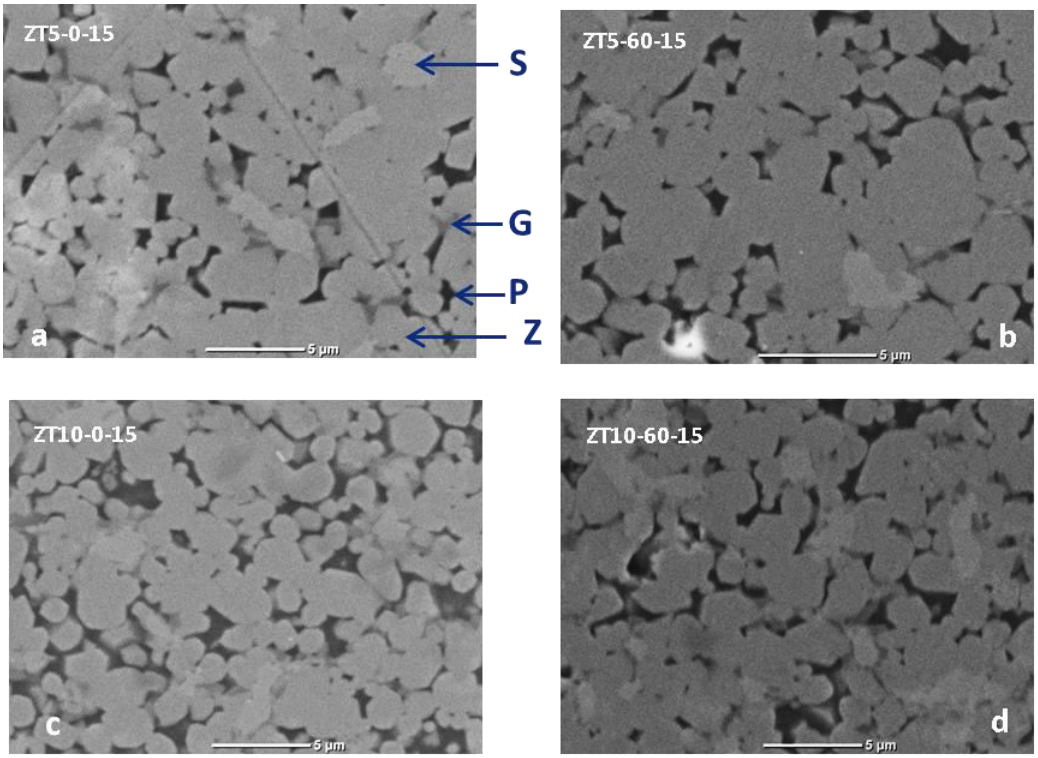

Fig. 7. SEM images of zircon – TiO_2 sintered ceramics (X2000 magnification) (see Table I for labels).

3.2.4. Mechanical properties, Hardness and fracture toughness

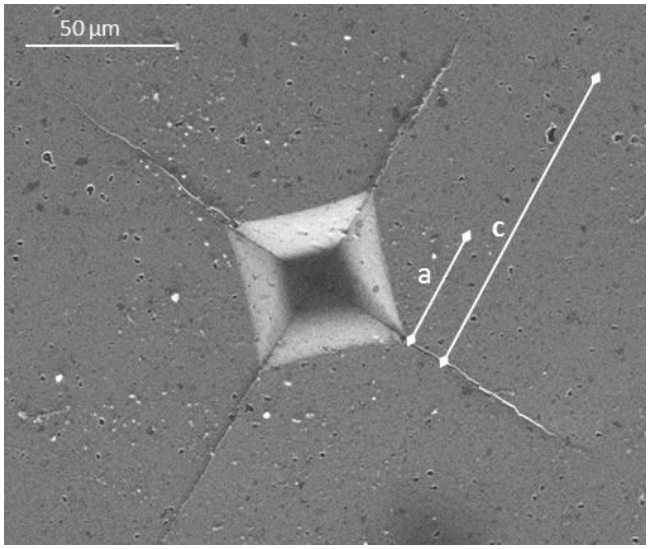

Fig. 8. Typical cracks of an indented sample in the developed ceramic materials.

Fig. 8 shows a SEM image with typical crack generated by an indentation in the studied materials. From the measurements of *a* and *c* parameters, applying the Equation 2, the fracture toughness of some of materials studied is determined, which are presented in Table V. The morphology of the observed cracks presents low tortuosity.

Tab. IV Comparison of Vickers hardness (Hv) of materials with data reported in literature and of the present study.

Sintering Process	Sintering Temp.	Matrix	Additive	Density	Vickers Hardness	Reference
	(^{o}C)		wt%	g.cm^{-3}	GPa (SD)	ref/ sample
C-Sol-Gel+ FCS	1500	$ZrSiO_4$	ZrO_2	4.4	10	[42]
H-Sol-Gel +FCS	1500	$ZrSiO_4$	ZrO_2	4.7	13	[42]
FCS	1600	$ZrSiO_4$	-	3.9	5.9	[43]
SPS	1300	$ZrSiO_4$	-	3.9	6.7	[43]
Milling + FCS	1600	$ZrSiO_4$	Al_2O_3 -10	3.8	6.3	[43]
Milling + SPS	1300	$ZrSiO_4$	Al_2O_3 -10	4.2	12.5	[43]
Milling + SPS	1300	$ZrSiO_4$	-	4.3	5.5	[10]
Milling + SPS	1400	$ZrSiO_4$	-	4.6	13.6	[10]
Milling + SPS	1500	$ZrSiO_4$	-	4.5	11.4	[10]
Milling + SPS	1300	$ZrSiO_4$	ZrO_2 -20	4.7	12.8	[11]
Milling + SPS	1400	$ZrSiO_4$	ZrO_2 - 20	4.8	14.8	[11]
Milling + SPS	1500	$ZrSiO_4$	ZrO_2 - 20	4.8	14.4	[11]
FCS	1600	$ZrSiO_4$	-	4.3	9.0 (2)	[14]
Milling + FCS	1600	$ZrSiO_4$	-	4.4	8.9 (2)	[14]
FCS	1400	$ZrSiO_4$	-	3.4	4.0 (2)	Z-0-14
FCS	1500	$ZrSiO_4$	-	4.0	5,5 (2)	Z-0-15
Milling +FCS	1400	$ZrSiO_4$	-	4.0	6.4 (2)	Z-60-14
Milling +FCS	1500	$ZrSiO_4$	-	4.3	8.4 (3)	Z-60-15
FCS	1400	$ZrSiO_4$	TiO_2 - 5	4.2	8.4 (2)	ZT5-0-14
Milling +FCS	1400	$ZrSiO_4$	TiO_2 - 5	4.4	10.0 (3)	ZT5-60-14
FCS	1500	$ZrSiO_4$	TiO_2 – 5	4.3	8.5 (3)	ZT5-0-15
Milling +FCS	1500	$ZrSiO_4$	TiO_2 – 5	4.4	8.9 (2)	ZT5-60-15
FCS	1500	$ZrSiO_4$	TiO_2 – 10	4.2	8.2 (3)	ZT10-0-15
Milling +FCS	1500	$ZrSiO_4$	TiO_2 – 10	4.3	8.5 (2)	ZT10-60-15

*C-Sol Gel: conventional process; H-Sol-Gel: Hydrothermal process; FCS: furnace conventional sintering technique; SPS: spark plasma sintering technique.

Hardness, can only be evaluated in pore free microstructures, with indents sufficiently larger than the material microstructure [36]. Fig. 9 shows the Hv values of the sintered materials as a

function of the relative density (%). A direct correlation can be observed in the studied range. Particularly, it can be assessed that dense materials fired at 1400 °C from milled powders present the highest hardness, being this value remarkably higher than the one of samples fired at 1500 °C. This material is well densified but the TiO_2 present did not react (see Fig. 5). Expectably, not fully sintered sample (Z-0-14) presents lower hardness, which restricts the actual application of this material as structural ceramics. The addition of new phases might affect the mechanical behavior of structural ceramics [25], as zirconia grains are involved in several toughening mechanisms [25, 26]. Apparently, $ZrTiO_4$ formation do not improves hardness of the zircon materials (TiO_2 added samples fired at 1500 °C).

The obtained values were compared with other dense zircon materials in Table IV. The achieved values correspond to dense zircon ceramics, and adequate for structural applications coupled with high refractoriness and special resistance to several severe chemical environments [37, 38] like other zircon based ceramics (Table IV). However, the achieved mechanical behavior is slightly below materials processes by more sophisticated routes like SPS [39, 40] or sol-gel derived materials [41]. While the first presents equipment and geometry restrictions, the second one presents, due to the usage of chemical precursors, environmental and scalability constraints, sustaining the merit of the present processing route.

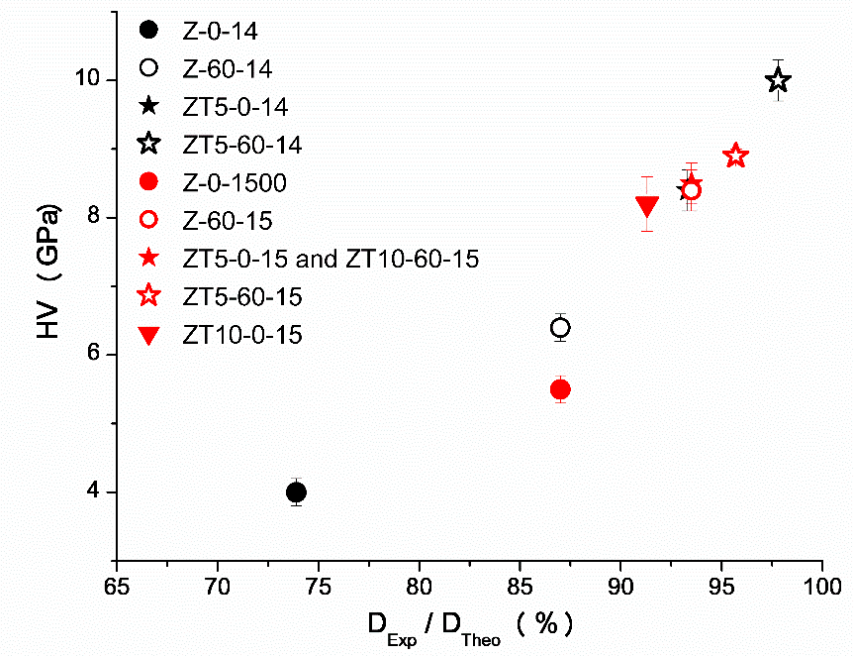

Fig. 9. Vickers hardness as a function of the relative density of the materials, for different sintering conditions, milling pretreatment and TiO_2 content.

Finally, Table V shows the Fracture Toughness (K_{IC}) of the zircon-titania based ceramics. Typically, fracture toughness of zircon ceramics is ranged between 2.0 and 3.5 $MPa.m^{-0.5}$ [10]. The achieved values are in the upper limit of the reported values. Apparently, materials fired at 1500 °C, fully dense and with a partial $ZrTiO_4$ formation presents slightly higher fracture toughness values. The multiphasic microstructure obtained might explain the toughening of the material [25, 26].

Hardness and toughness values obtained show the merits of the materials processed in the present study. While resulting density is comparable with the best figures reported, hardness and fracture toughness achieved were as high as any pure dense zircon material.

Tab. V Fracture Toughness (K_{IC}) of the $ZrSiO_4$ - TiO_2 bases studied materials.

Sample	Sintering Process	Sintering Temp.	Matrix phase	TiO_2 initial Addition	K_{IC}
		°C		wt%	MPa.m$^{0.5}$ (SD)
ZT5-0-14	FCS	1400	$ZrSiO_4$	5	1.8 (2)
ZT5-60-14	Milling +FCS	1400	$ZrSiO_4$	5	1.9 (4)
ZT5-0-15	FCS	1500	$ZrSiO_4$	5	1.8 (2)
ZT5-60-15	Milling +FCS	1500	$ZrSiO_4$	5	2.2 (1)
ZT10-0-15	FCS	1500	$ZrSiO_4$	10	2.4 (3)
ZT10-60-15	Milling +FCS	1500	$ZrSiO_4$	10	2.3 (3)

*FCS: furnace conventional sintering

4. Conclusion

The effect of the TiO_2 addition in the ceramic processing of dense zircon ceramics from fine zircon powders was established. For this, a systematic formulation - processing - properties study was carried out. The sintering parameters were evaluated; their effect in the sintering was established. Both milling and TiO_2 addition (up to 10 wt.%) enhance de zircon fine powders consolidation.

The thermochemical processes were described in terms of the processing variables: formulation and heating programs; homogenous dense microstructures were achieved.

The addition of TiO_2 permitted to obtain dense ceramics at lower temperatures around 100-150 °C below, with comparable mechanical behavior, without employing any sophisticated processing route, like sol-gel derived ceramics or electric current activated sintering strategies like SPS. The thermochemical processes were described. After 1400 °C heating programs, added TiO_2 acts as a sintering aid with no important chemical reactions, these samples presented the better mechanical behavior. On the other side in samples fired at 1500 °C, TiO_2 partially (≈ 50 %) reacts with zircon forming $ZrTiO_4$, the formed SiO_2 goes to the grain boundaries.

Remarkably, samples with 5 wt% TiO_2 present better mechanical behavior than the 10 wt% samples. The mechanical characterization shows the merits of the material processed in the present study. While resulting density is comparable with the best figures reported; the hardness and fracture toughness achieved were as high as any pure dense zircon material.

Acknowledgments

JMM acknowledges CONICET for the fellowships; this work was partially financed by ANPCyT (PICT-2016-1193) and CONICET (PIO CONICET-UNLA 2016-2018. No. 22420160100023), and UNLP (2015-2018 X-737).; MG, GS and NMR are members of the CONICET.

5. References

1. A. Kaiser, M. Lobert, R. Telle, Thermal stability of zircon (ZrSiO4), J. Eur. Ceram. Soc. 28 (2008) 2199-2211.
2. Satoshi Koshimizu, Comparison of thermal stability between internal and external surfaces of zircon, Nucl. Tracks Radiat. Meas. 22 (1993) 785-788.

3. A. M. Evans, J. P. H. Williamson, F. P. Glasser, Microstructure of plasma dissociated zircon and liquid immiscibility in the ZrO_2-SiO_2 system, J. Mater. Sci. 15 (1980) 2325-2330.
4. N. E. Timms, T. M. Erickson, M. A. Pearce, A. J. Cavosie, M. Schmieder, E. Tohver, S. M. Reddy, M. R. Zanetti, A. A. Nemchin, A. Wittmann, A pressure-temperature phase diagram for zircon at extreme conditions, Earth-Sci. Rev. 165 (2017) 185-202.
5. N. M. Rendtorff, L. B. Garrido, E. F. Aglietti, Thermal shock resistance and fatigue of Zircon–Mullite composite materials, Ceram. Int. 37 (2011) 1427-1434.
6. I. G. Mel'nikova, T. A. Nesterova, I. V. Razdol'skaya, Zircon refractories for glass-melting (review), Glass Ceram. 42 (1985) 295-298.
7. M. Awaad, S. H. Kenawy, Sintering of zircon: the role of additives, Br. Ceram. Trans. 102 (2003) 69-72.
8. Y. Shi, X. Huang, D. Yan, Fabrication of hot-pressed zircon ceramics: Mechanical properties and microstructure, Ceram. Int. 23 (1997) 457-462.
9. S. Huang, Q. Li, Z. Wang, X. Cheng, H. Wen, Effect of sintering aids on the microstructure and oxidation behavior of hot-pressed zirconium silicate ceramic, Ceram. Int. 43 (2017) 875-879.
10. N. M. Rendtorff, Salvatore. Grasso, C. Hu, G. Suarez, E. F. Aglietti, Y. Sakka, Dense zircon ($ZrSiO_4$) ceramics by high energy ball milling and spark plasma sintering, Ceram. Int. 38 (2012) 1793-1799.
11. N. M. Rendtorff, S. Grasso, C. Hu, G. Suarez, E. F. Aglietti, Y. Sakka, Zircon–zirconia ($ZrSiO_4$–ZrO_2) dense ceramic composites by spark plasma sintering, J. Eur. Ceram. Soc. 32 (2012) 787-793.
12. C. Suryanarayana, Mechanical alloying and milling, Prog. Mater. Sci. (2001) 184.
13. W.-S. Jung, H.-S. Park, Y. J. Kang, D.-H. Yoon, Lowering the sintering temperature of Gd-doped ceria by mechanochemical activation, Ceram. Int. 36 (2010) 371-374.
14. M. Gauna, M. Conconi, G. Suarez, E. Aglietti, N. Rendtorff, Dense zircon ($ZrSiO_4$) ceramics by a simple milling-sintering route, Sci. Sinter. 50 (2018) 15-28.
15. S. Motoi, Mechanochemical effect in zircon by mechanical grinding, J Ceram Soc Jpn. 86 (1978) 92-95.
16. S. Ghaffari, K. Asadian, T. Ebadzadeh, M. Alizadeh, A. Ghanbari, Effects of milling and subsequent heat treatment on preparation of mullite–zirconia nanocomposites, Micro Amp Nano Lett. 8 (2013) 193-196.
17. R. Emadi, H. Ashrafi, R. Zamani Foroushani, Effect of temperature on the reaction sintering of mechanically activated $ZrSiO_4$–Al_2O_3 mixture, Ceram. Int. 41 (2015) 14400-14405.
18. G. Suárez, S. Acevedo, N. M. Rendtorff, L. B. Garrido, E. F. Aglietti, Colloidal processing, sintering and mechanical properties of zircon ($ZrSiO_4$), Ceram. Int. 41 (2015) 1015-1021.
19. J. Wei, B. Han, W. Zhou, X. Xiang, W. Yan, Y. Wei, J. Chen, N. Li, Fabrication of double-decker zircon aggregates by granulation and influence of TiO_2 on the sintering process, Ceram. Int. 46 (2020) 3412-3419.
20. E. López-López, J. P. Erauw, R. Moreno, C. Baudín, F. Cambier, Elastic behaviour of zirconium titanate bulk material at room and high temperature, J. Eur. Ceram. Soc. 32 (2012) 4083-4089.
21. E. López-López, C. Baudín, R. Moreno, I. Santacruz, L. Leon-Reina, M. A. G. Aranda, Structural characterization of bulk $ZrTiO_4$ and its potential for thermal shock applications, J. Eur. Ceram. Soc. 32 (2012) 299-306.
22. A. George, S. Solomon, J. K. Thomas, A. John, Characterizations and electrical properties of $ZrTiO_4$ ceramic, Mater. Res. Bull. 47 (2012) 3141-3147.

23. N. M. Rendtorff, S. Gómez, M. R. Gauna, M. S. Conconi, G. Suarez, E. F. Aglietti, Dense mullite–zirconia–zirconium titanate ceramic composites by reaction sintering, Ceram. Int. 42 (2016) 1563-1572.
24. M. A. Violini, M. F. Hernández, M. Gauna, G. Suarez, M. S. Conconi, N. M. Rendtorff, Low (and negative) thermal expansion Al_2TiO_5 materials and Al_2TiO_5 - $3Al_2O_3{\cdot}2SiO_2$ - $ZrTiO_4$ composite materials. Processing, initial zircon proportion effect, and properties, Ceram. Int. 44 (2018) 21470-21477.
25. T. Ohji, Y.-K. Jeong, Y.-H. Choa, K. Niihara, Strengthening and Toughening Mechanisms of Ceramic Nanocomposites, J. Am. Ceram. Soc. 81 (2005) 1453-1460.
26. N. M. Rendtorff, L. B. Garrido, E. F. Aglietti, Zirconia toughening of mullite–zirconia–zircon composites obtained by direct sintering, Ceram. Int. 36 (2010) 781-788.
27. Y. Shi, X. Huang, D. Yan, Toughening of hot-pressed ZrSiO4 ceramics by addition of Y-TZP, Mater. Lett. 35 (1998) 161-165.
28. M. R. Gauna, M. S. Conconi, S. Gomez, G. Suárez, E. F. Aglietti, N. M. Rendtorff, Monoclinic - tetragonal zirconia quantification of commercial nanopowder mixtures by XRD and DTA, (2015) 9.
29. H. M. Rietveld, A profile refinement method for nuclear and magnetic structures, J. Appl. Crystallogr. 2 (1969) 65-71.
30. D. L. Bish, S. A. Howard, Quantitative phase analysis using the Rietveld method, J. Appl. Crystallogr. 21 (1988) 86-91.
31. R. J. Moreira Toja, N. M. Rendtorff, E. F. Aglietti, T. Uchikoshi, Y. Sakka, G. Suárez, Influence of the porosity caused by incomplete sintering on the mechanical behaviour of lanthanum silicate oxyapatite, Ceram. Int. 44 (2018) 14348-14354.
32. S. Filipović, N. Obradović, S. Marković, A. Đorđević, I. Balać, A. Dapčević, J. Rogan, V. Pavlović, Physical properties of sintered alumina doped with different oxides, Sci. Sinter. 50 (2018) 409-419.
33. D. L. Bish, J. E. Post, Quantitative mineralogical analysis using the Rietveld full-pattern fitting method, Am. Mineral. 78 (1993) 932-940.
34. A. G. Evans, E. A. Charles, Fracture Toughness Determinations by Indentation, J. Am. Ceram. Soc. 59 (1976) 371-372.
35. J. Vujančević, A. Bjelajac, J. Ćirković, V. Pavlović, E. Horvath, L. Forró, B. Vlahović, M. Mitrić, Đ. Janaćković, V. Pavlović, Structure and photocatalytic properties of sintered TiO_2 nanotube arrays, Sci. Sinter. 50 (2018) 39-50.
36. J. Gong, J. Wu, Z. Guan, Examination of the Indentation Size E€ ect in Low-load Vickers Hardness Testing of Ceramics, (n.d.) 7.
37. C. B. Carter, M. G. Norton, Ceramic materials: science and engineering, Springer, New York, 2007.
38. C. Baudín, Processing of Alumina and Corresponding Composites, in: Compr. Hard Mater., Elsevier, 2014: pp. 31-72.
39. R. Chaim, M. Levin, A. Shlayer, C. Estournes, Sintering and densification of nanocrystalline ceramic oxide powders: a review, Adv. Appl. Ceram. 107 (2008) 159-169.
40. S. Grasso, Y. Sakka, G. Maizza, Electric current activated/assisted sintering (*ECAS*): a review of patents 1906–2008, Sci. Technol. Adv. Mater. 10 (2009) 053001.
41. A. K. Mishra, ed., Sol-gel Based Nanoceramic Materials: Preparation, Properties and Applications, Springer International Publishing, Cham, 2017.
42. Y. Ding, Z. Jiang, Y. Li, Y. Tang, J. Li, X. Dong, H. Dan, Y. Yang, T. Duan, Low temperature and rapid preparation of zirconia/zircon ($ZrO_2/ZrSiO_4$) composite ceramics by a hydrothermal-assisted sol-gel process, J. Alloys Compd. 735 (2018) 2190-2196.

43. M. C. Anjali, P. Biswas, D. Chakravarty, U. S. Hareesh, Y. S. Rao, R. Johnson, Low temperature in-situ reaction sintering of zircon: Alumina composites trough spark plasma sintering, Sci. Sinter. 44 (2012) 323-330.

Сажетак: *Утврђен је утицај додатка TiO_2 у процесирање густе цирконијумске керамике из финог праха цирконијума. Додатак TiO_2 (5-10 wt%) омогућио је добијање густе керамике на нижим температурама (ниже за 100-150 ^oC), са компаративним механичким својствима. Термо-хемијски процеси су описани након неколико експерименталних техника, као што су синтеровање, рендгенска дифракција, скенирајућа електронска микроскопија и Викерсова тврдоћа рађена на исполираним густим узорцима. После синтеровања на 1400 ^oC, додатак TiO_2 се понаша као помоћно средство без значајних хемијских реакција, и представља побољшање у механичким својствима у поређењу са чистом цирконијумском керамиком. Са друге стране, у узорцима синтерованим на 1500 ^oC, TiO_2 делимично (≈ 50 %) реагује са цирконујумом, формирајући $ZrTiO_4$, док SiO_2 одлази на границе зрна. Узорци са 5 wt% TiO_2 показују боља механичка својства од узорака са 10 wt%. Испољена механичка својства показују оправданост овог материјално исплативог процеса. Добијена густина, тврдоћа (≈10 GPa) и жилавост лома (≈ 2 MPa.$m^{-1/2}$) су упоредиви са литературним подацима.*
Кључне речи*: цирконијум, TiO_2, процесирање, синтеровање, својства.*